

Supporting Information

Plasmon of Au Nanorods Activates Metal-Organic Frameworks for both Hydrogen Evolution Reaction and Oxygen Evolution Reaction

Wenmin Zhang,^{§a} Shanshan Wang,^{§bc} Shengyuan A. Yang,^b Xing-Hua Xia^d, and Yi-Ge Zhou^{*a}

Experimental Procedures

Instrumentation. Powder X-ray diffraction (PXRD) patterns were obtained on a D8 Advance X-ray diffractometer (Bruker, Germany) with the Cu K α irradiation source ($\lambda = 1.54056 \text{ \AA}$). The morphology of samples was characterized by transmission electron microscopy (TEM, JEOL-2010, Japan) supported on a carbon film. Scanning electron microscopic (SEM) images were acquired on silicon wafers by a Hitachi S-4800. Atomic force microscopy (AFM) measurements were carried out on a Bruker multimode-8 scanning probe microscope. XPS spectra were obtained on a PHI 5000 VersaProbe (Japan) instrument. The binding energy was calibrated by means of the C 1s peak energy of 284.6 eV. The contents of Au in the composites were quantified by an Optima 7300 DV inductively coupled plasma-mass (ICP-MS). Zeta potentials for AuNRs, Co-MOFNs and AuNRs/Co-MOFNs composites were measured by Malvern Zetasizer ZEN3600. The UV-vis absorption spectra were obtained on a UV-visible spectrophotometer (UV-2600, Shimadzu Corp). All electrochemical measurements were conducted on an Autolab PGSTAT204 electrochemical analyzer (Metrohm, Nethedands).

Reagent. All chemicals were obtained from commercial sources and used without further purification. Nickel(II) chloride hexahydrate ($\text{NiCl}_2 \cdot 6\text{H}_2\text{O}$, >99.9%), Cobalt(II) chloride hexahydrate ($\text{CoCl}_2 \cdot 6\text{H}_2\text{O}$, >99.9%) and sodium oleate (NaOL, >97.0%) were purchased from Sinopharm Chemical Reagent. Benzenedicarboxylic acid (H_2BDC), hexadecyl trimethyl ammonium bromide (CTAB, >98.0%), L-ascorbic acid (AA, $\geq 99.5\%$), silver nitrate (AgNO_3 , >99.0%), sodium citrate (>99.0%), hydrogen tetrachloroaurate trihydrate ($\text{HAuCl}_4 \cdot 3\text{H}_2\text{O}$, $\geq 99.5\%$), sodium borohydride (NaBH_4 , 99.0%), and hydrochloric acid (HCl, 37 wt.% in water) were obtained from Sigma Aldrich. Nafion solution (0.5 wt.%), KOH (99.8%) and H_2SO_4 (99.0%) were purchased from Alfa Aesar. Triethylamine (TEA), N, N-dimethylformamide (DMF) and ethanol were obtained from Aladdin Reagent. Ultrapure water (resistivity of 18.2 M Ω -cm) used in the experiments was supplied by a Millipore System (Millipore Q).

Synthesis of Co-, Ni- and NiCo-MOFNs. The Co-MOFNs was synthesized according to the procedures reported previously with minor modifications.¹ Firstly, ethanol (2 mL), water (2 mL) and DMF (32 mL) were mixed in a 100 mL Erlenmeyer flask. Secondly, 0.750 mmol H_2BDC was dissolved into the mixed solution under magnetic stirring. Subsequently, 0.750 mmol $\text{CoCl}_2 \cdot 6\text{H}_2\text{O}$ was added and allowed to stir continuously until Co^{2+} salts was dissolved completely. A 0.8 mL TEA was then quickly injected into the solution, followed by stirring for a few minutes to obtain a uniform colloidal suspension. Afterwards, the colloidal solution was continuously ultrasonicated for 10 h (40 kHz) under airtight conditions. After washing by centrifugation in ethanol for 5 times, the products were finally obtained and dried at room temperature. The preparation procedures of Ni-MOFNs and NiCo-MOFNs were the same as that of Co-MOFNs, except that 0.750 mmol Co^{2+} was replaced by 0.375 mmol Ni^{2+} and 0.375 mmol Co^{2+} for NiCo-MOFNs.

Synthesis of AuNRs. Before synthesis, all glassware was cleaned with freshly prepared aqua regia (HCl:HNO₃ in a 3:1 ratio by volume) followed by ultrasonic cleaning four times with water.

Seed solution of AuNRs was prepared according to the procedure reported elsewhere.² A 0.250 mL 0.010 mM HAuCl_4 was mixed with 7.5 mL 0.100 M CTAB solution in a 15 mL centrifuge tubes by oscillation till the solution turned yellow. Afterwards, 0.6 mL fresh NaBH_4 (0.01 M) was quickly injected into the seed solution under vigorous stirring (1200 rpm). The stirring was terminated after 2 min when the solution color changed from yellow to brownish-yellow. The seed solution was aged at room temperature for 2 h before use.

The growth solution was prepared according to the procedure reported previously. Typically, 7.0 g CTAB and 1.234 g NaOL were dissolved in 250 mL water (*ca.* 50 °C) in a 1 L Erlenmeyer flask and stirred until they were completely dissolved. The solution was allowed to cool down at room temperature before 18.0 mL 4 mM AgNO_3 solution was added. The mixture was kept undisturbed at room temperature for 20 min after 250 mL 1 mM HAuCl_4 solution was added. The solution became colorless after several minutes of stirring (1000 rpm) and 1.5 mL HCl (37 wt.% in water, 12.1 M) was then introduced to adjust the pH. After 15 min of slow stirring at 700 rpm, 1.25 mL 0.064 M AA was added and the solution was vigorously stirred for several seconds. Finally, 0.4 mL seed solution was injected into the growth solution. The resulting mixture was stirred for one minute and left undisturbed at 30 °C for 12 h for gold nanorods growth. The final products were isolated by centrifugation at 11,000 rpm for 20 min followed by the removal of the unbound CTAB for three times. After that the supernatant was discarded, and the precipitate was redispersed in 10 mL of Milli-Q water.

Synthesis of AuNSs. AuNSs were prepared according to the procedure reported.³ Briefly, 150 mL of 0.01 wt.% HAuCl_4 was prepared in the 250 mL Bottom flask and heated to boiling, then 5 mL of 1 wt.% sodium citrate was added under vigorous stirring for 10 min. The color of the solution changed from yellow to wine red.

Preparation of AuNRs/AuNSs modified Co-MOFNs composites (AuNRs/Co-MOFNs and AuNSs/Co-MOFNs composites). The AuNRs/Co-MOFNs composites were prepared by mixing both the AuNRs after removing excess of CTAB with large amount of water and Co-MOFNs solutions with a volume ratio of 1:1. The mixture was then sonicated for more than two hours with a commercial ultrasonic cleaner. After that, the precipitates were separated by centrifugation and dried in an oven at 50 °C under vacuum overnight. The preparation procedures of AuNSs/Co-MOFNs composites, AuNRs/Ni-MOFNs and AuNRs/NiCo-MOFNs composites were the same as that of AuNRs/Co-MOFNs.

Electrochemical Characterization. Electrochemical measurements were conducted on a three-electrode system at room temperature. A 3 mm diameter glassy carbon electrode modified with the catalyst was used as a working electrode. A graphite rod and Pt wire were used as the counter electrode for HER and OER, respectively, and an Ag/AgCl electrode was used as the reference. All the potentials were calibrated to the reversible hydrogen electrode (RHE) using the following equation: $E_{\text{RHE}} = E_{\text{Ag/AgCl}} + 0.197 \text{ V} + 0.059 \text{ pH}$. The catalyst was dispersed and sonicated in 0.5 mL 0.5 wt.% Nafion solution for 5 min before drop cast on a glassy carbon electrode and dried at room temperature. All electrochemical scans were collected using linear sweep voltammetry at a scan rate of 50 mV/s. Tafel plots were recorded

with the linear portions at low overpotential fitted to the Tafel equation ($\eta = b \log j + a$, where η is overpotential, j is the current density, and b is the Tafel slope). All the electrochemical data were presented without iR -correction. Electrochemical impedance spectroscopy (EIS) measurements were carried out from 100000 Hz to 1 Hz with an amplitude of 10 mV.

Electrical Characterization: The I - V curves of AuNRs/Co-MOFNs were performed on semiconductor parameter analyzer (2634B, Keithley).

Computational Details. The ab-initio calculations were implemented with Vienna ab initio simulation package (VASP) based on the framework of density functional theory (DFT) within the projector-augmented wave method.⁴ The generalized gradient approximation (GGA) with the Perdew-Burke-Ernzerhof (PBE) was adopted to describe the electron exchange-correlations interactions.^{5,6} A cutoff energy of 500 eV was employed for the plane wave expansion of the wave function. Lattice constants were fixed in the calculations, while the atom positions were relaxed. Considering the Co (3d) orbitals may present strong correlation effect, GGA+U method was used in electronic structure calculations,^{7,8} with the on-site Hubbard U of 4 eV for Co atoms.

The surface was modelled by the (001) plane of our UMOFNs. In Figure S14, (a) is the schematic figure of UMOFNs and (b) presents the 2D slab model used in our calculations, which is highlighted with the light blue shadow. The lattice constants are 6.295 Å and 19.9337 Å. A sufficiently large vacuum region of 20 Å along c axis was used to avoid the artificial interactions between layers. The Brillouin-zone was sampled with $7 \times 7 \times 1$ Monkhorst-Pack k -mesh for atom position optimizations in 2D slab,⁹ and the force convergence criterion was set to 0.05 eV/Å. The energy convergence criterion was 10^{-5} eV. For projected density of states calculations, a denser k -mesh $10 \times 15 \times 1$ was adopted. The cell used in calculations belongs to space group P_2 . The corresponding high symmetry points and k -path are shown in Figure S14 (c) denoted by the black solid lines.

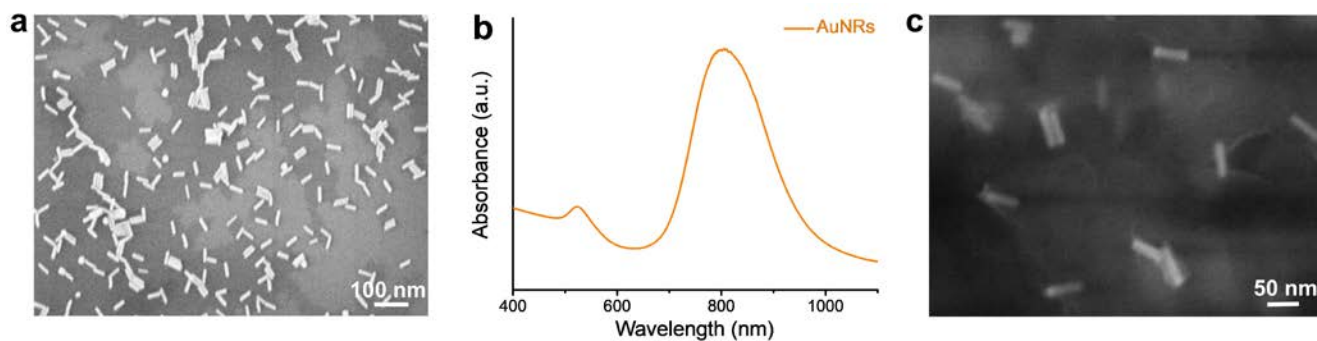


Figure S1. SEM characterization (a) and UV-vis absorption spectrum (b) of AuNRs. SEM characterization of AuNRs/Co-MOFNs composites (c).

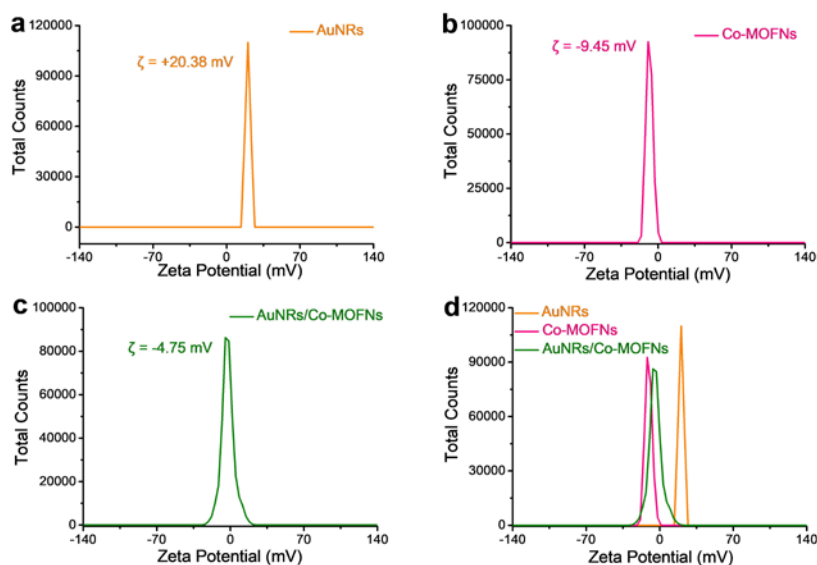


Figure S2. Zeta potentials of AuNRs (a), Co-MOFNs (b) and AuNRs/Co-MOFNs (c) and overlay profile (d) determined when dispersed in a water/ethanol (1:1 volume ratio) mixture solution.

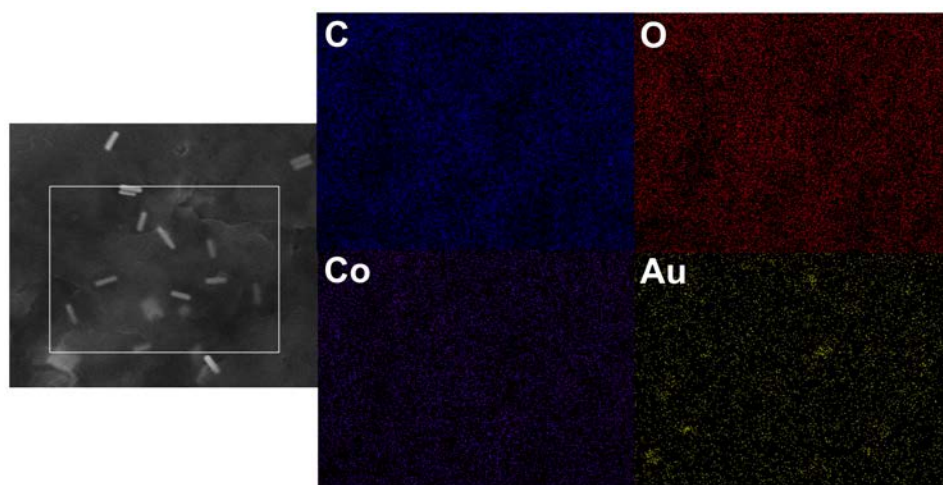


Figure S3. Elemental mapping of C (blue), O (red), Co (purple) and Au (yellow) at AuNRs/Co-MOFNs in the selected area.

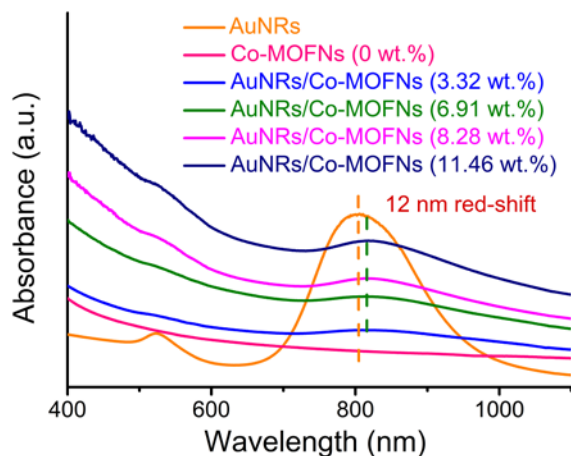


Figure S4. UV-vis absorption of AuNRs/Co-MOFNs composites with different loading density of AuNRs.

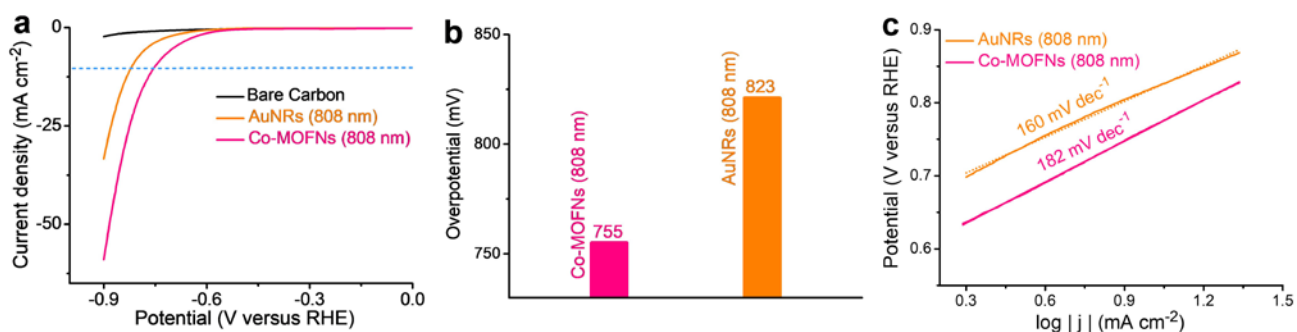


Figure S5. (a) HER polarization curves obtained on a bare glassy carbon (black line), AuNRs (orange line) and Co-MOFNs (pink line) in 0.5 M H_2SO_4 electrolyte with 808 nm light irradiation. (b) Comparison of overpotentials (η) at the current density of 10 mA cm^{-2} (indicated by light blue dashed line) for AuNRs (orange column) and Co-MOFNs (pink column) with 808 nm light irradiation. (c) Tafel curves of AuNRs (orange line) and Co-MOFNs (pink line) with 808 nm light irradiation.

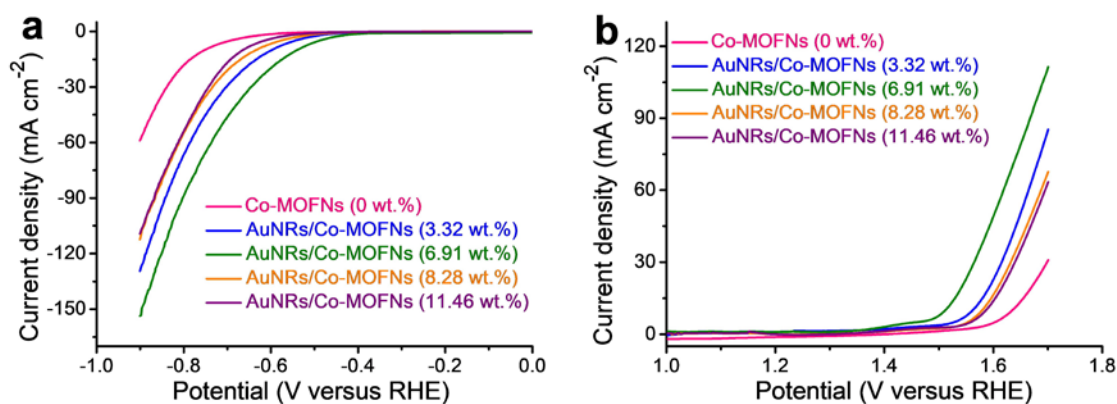


Figure S6. HER(a) and OER(b) polarization curves of AuNRs/Co-MOFNs composites with different AuNRs loadings measured under 808 nm light.

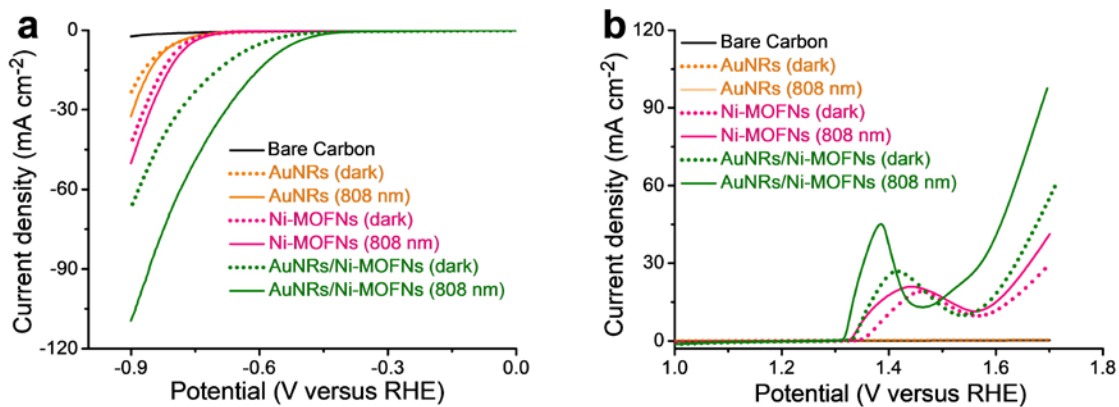


Figure S7. HER (a) and OER (b) polarization curves obtained on AuNRs (orange line), Ni-MOFNs (pink line) and AuNRs/Ni-MOFNs composites (green line) with (solid line) and without (dotted line) 808 nm light irradiation.

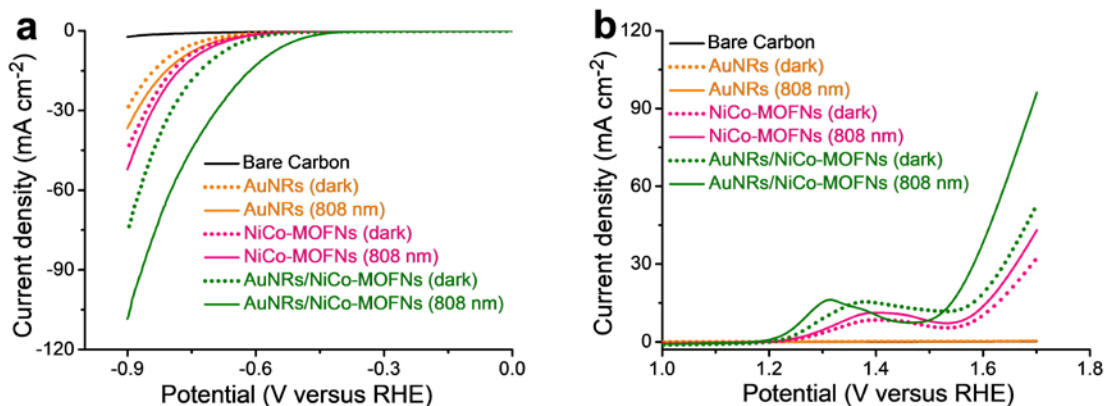


Figure S8. HER (a) and OER (b) polarization curves obtained on AuNRs (orange line), NiCo-MOFNs (pink line) and AuNRs/NiCo-MOFNs composites (green line) with (solid line) and without (dotted line) 808 nm light irradiation.

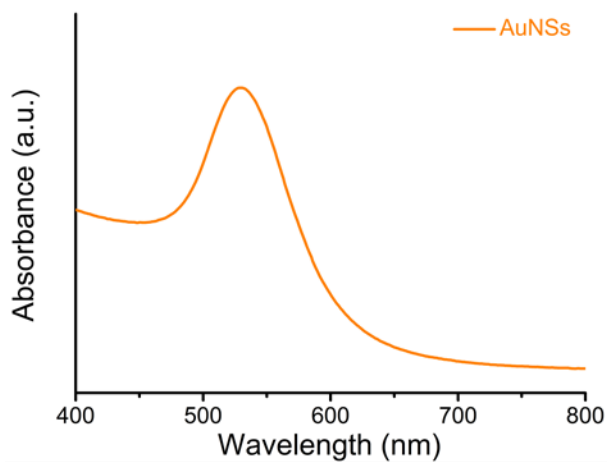


Figure S9. UV-vis absorption spectrum of AuNSs.

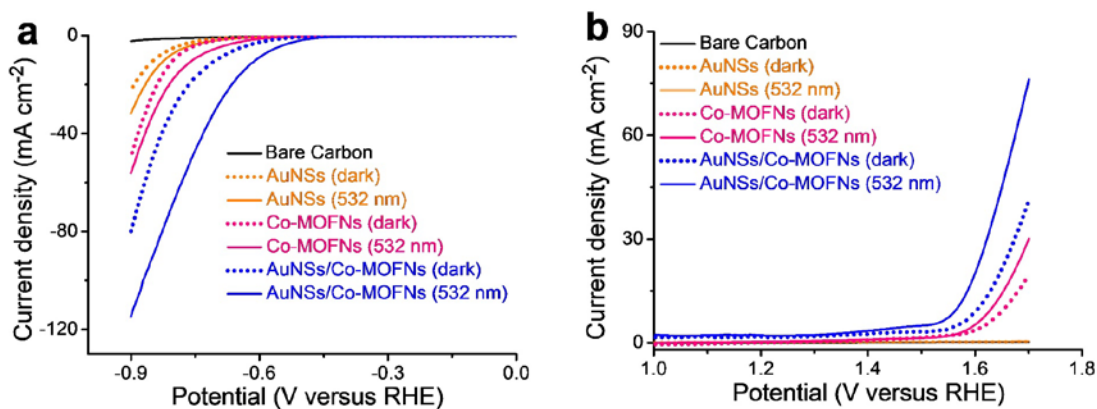


Figure S10. (a) HER and (b) OER polarization curves obtained on AuNSs (orange line), Co-MOFNs (pink line) and AuNSs/Co-MOFNs composites (blue line) with (solid line) and without (dotted line) 532 nm light irradiation.

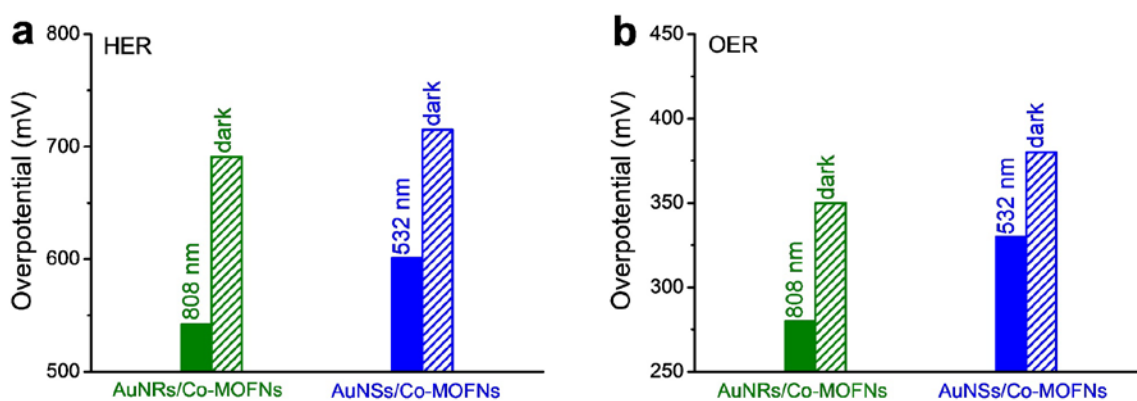


Figure S11. Comparison of overpotentials (η) at the current density of 10 mA cm^{-2} at AuNRs/Co-MOFNs (green column) and AuNSs/Co-MOFNs (blue column) with (solid) and without (patterned) light irradiation toward HER (a) and OER (b).

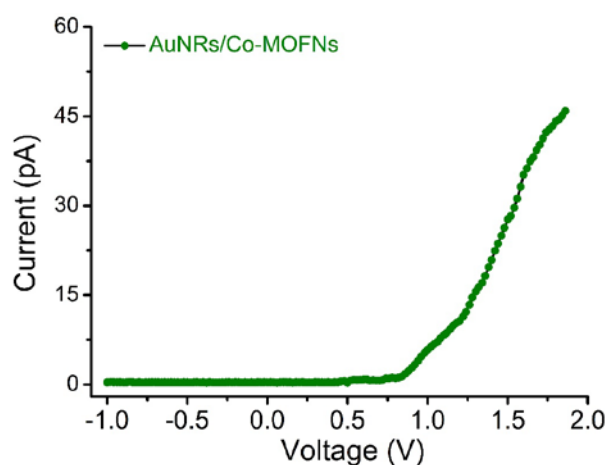


Figure S12. I - V curve of AuNRs/Co-MOFNs composites, confirming the existence of Schottky barrier.

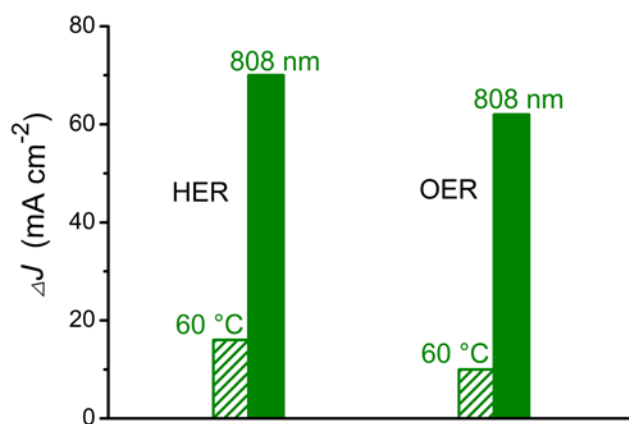


Figure S13. Current density increase compared with that obtained at 25 °C under dark for HER and OER on AuNRs/Co-MOFNs composites at 25 °C under 808 nm light irradiation (solid column) and 60 °C under dark (patterned column).

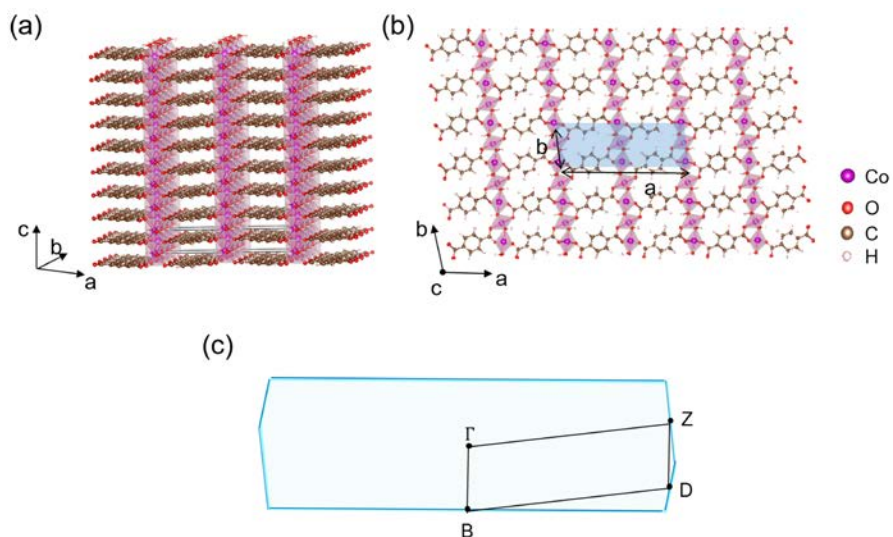


Figure S14. Schematic figures of MOFNS and slab model. (a) Structure of MOFNS with purple denoting Co atom, red denoting O atom, brown denoting C atom and light grey denoting H atom. (b) 2D MOFNS slab with light blue shadow indicating the super cell used in calculations, a and b are lattice constants. (c) Brillouin zone with k-path for band structure calculation.

References

- 1 S. L. Zhao, Y. Wang, J. C. Dong, C. T. He, H. J. Yin, P. F. An, K. Zhao, X. F. Zhang, C. Gao, L. J. Zhang, J. W. Lv, J. X. Wang, J. Q. Zhang, A. M. Khattak, N. A. Khan, Z. X. Wei, J. Zhang, S. Q. Liu, H. J. Zhao and Z. Y. Tang, *Nat. Energy.*, 2016, **1**, 16184.
- 2 X. Ye, C. Zheng, J. Chen, Y. Z. Gao and C. B. Murray, *Nano Lett.*, 2013, **13**, 765-771.
- 3 G. Frens, *Nature Phys. Sci.*, 1973, **241**, 20-22.
- 4 G. Kresse and J. Furthmueller, *Phys. Rev. B.*, 1996, **54**, 11169-11186..
- 5 J. P. Perdew, K. Burke and M. Ernzerhog. *Phys. Rev. Lett.*, 1996, **77**, 3865-3868.
- 6 G. Kresse and D. Joubert, *Phys. Rev. B.*, 1999, **59**, 1758-1775.
- 7 V. I. Anisimov, I. V. Solowyev and M. A. Korotin. *Phys. Rev. B.*, 1992, **48**, 16929-16934.
- 8 V. I. Anisimov, F. Aryasetiawan and A. I. Lichtenstein. *J. Phys.: Condens. Matter.*, 1997, **9**, 767-808.
- 9 H. J. Monkhorst and J. D. Pack. *Phys. Rev. B.*, 1976, **13**, 5188-5192.